Internal feedback enables rapid trajectory control during goal-directed finger and whole-arm reaching movements

Niranjan Chakrabhavi [a,b,*], Varadhan SKM [b], Ashitava Ghosal [c], Aditya Murthy [a,*]

[a]Centre for Neuroscience, Indian Institute of Science, Bengaluru 560012, India. [b]Department of Applied Mechanics, Indian Institute of Technology Madras, Chennai 600036, India. [c]Department of Mechanical Engineering, Indian Institute of Science, Bengaluru 560012, India.

[*]Corresponding Authors – Niranjan Chakrabhavi (niranjanc@iisc.ac.in) and Aditya Murthy (adi@isc.ac.in).

Author Contribution: NC conceived the study; NC and VSKM designed the finger experiment; NC and AM designed the arm experiment; NC collected data and performed the data analysis; AM and AG supervised the analysis; NC and AM wrote the manuscript; AG and VSKM reviewed the manuscript.

Competing Interest Statement: The authors declare no competing interest.

Classification: Major – Biological Sciences, Minor – Neuroscience.

Keywords: motor control, trajectory planning, variability, and decorrelation.

This pdf file includes:

1. Main text
2. Figures 1 to 4

Supporting Information: This article contains supporting information.

Abstract

Goal-directed behaviors involve the execution of a variety of eye, hand, and finger movements that follow invariant kinematics consisting of straight-line trajectories and bell-shaped velocity profiles, despite the presence of neuromotor noise and distinct biomechanics. A fundamental unresolved issue in the field is to determine and delineate the extent to which these trajectories are planned or whether trajectories are a consequence of online control. In this study, we addressed this question using a unitless geometric measure along with the rate of zero-crossings to analyze within-trial variability to investigate differences in the time course of trajectories during the presence or absence of a goal in finger and whole-arm reaching movements. We found that the CNS implements control to follow an average trajectory, where the goal-directed movements showed an enhanced degree of trajectory control than the non-goal movements. Further, by performing the analysis on the actual timing, we found behavioral signatures of internal feedback control that might operate on these planned trajectories as early as 30 ms in finger movements and 16.6 ms in whole-arm reach movements. The analysis also revealed that the controller gains varied along the movement and peaked distinctly at early (20%) and late (90%) phases of movement, suggesting that the CNS breaks down the movement into accomplishing virtual way-point objectives during the execution of movement.

Significance Statement

The extent to which movements reflect the unfolding of a prespecified trajectory plan or whether trajectories arise from the characteristics of online control has remained a vexing issue for motor theorists. Using novel metrics of control (decorrelation and zero-crossing rate) and a novel comparison between goal and non-goal conditions in finger and whole-arm reaching movements, we demonstrate that the CNS implements rapid internal feedback control to follow

a planned trajectory. Interestingly, the extent of trajectory control was not continuous but was implemented in distinct stages at the early and late phases of movement. Taken together these results provide novel constraints for computational theories of motor control.

Introduction

Normative goal-directed movements are characterized by invariant-kinematic patterns that consist of straight-line trajectories with bell-shaped velocity profiles that scale with movement amplitude and speed (1). Numerous psychophysical and neurophysiological studies highlight the notion that movement attributes are represented/programmed in the central nervous system well before execution (2–10). Such results have motivated the use of internal models wherein a complete specification of a trajectory can be made, in principle, before its implementation (11–15). However, other influential models of motor control suggest that only certain critical features of the movement such as the endpoint or desired displacement need to be specified in advance (16–18); here, the neural representation specifying movement trajectories may only be generated dynamically in real-time during movement execution as a consequence of sensory feedback that is sensitive to the demands of the task. Thus, it remains unclear whether movement attributes such as trajectories are planned prior to movement execution or whether they derive from online feedback control.

One feature that in principle can distinguish between planned and derived movement trajectories is the timing of their respective control signals that are necessary to mitigate the effects of motor noise that is a ubiquitous property of muscle and neural activity. Whereas in the context of planned movement trajectories, fast internal feedback control is posited to use an efference copy of the planned motor command to make predictions on the sensory

consequences (internal feedback) to control movements in the absence of actual sensory information (19–21). In contrast, sensory feedback control relies on relatively delayed sensory (> 50 ms) feedback to make meaningful corrections during the movement (22, 23). While internal feedback back control has been extensively studied in fast saccadic eye movements (21, 24, 25) distinct signatures of such control in the context of normative arm movements in the absence of sensory perturbations have not been experimentally demonstrated.

Using the distinction between the temporal properties of these two forms of control, we used a novel unitless-geometric approach and compared the profiles in movements which were either goal/task driven versus a similar movement in the absence of a goal/task to determine whether trajectory control is based exclusively on sensory feedback (26, 27) or can it also involve internal feedback control as predicted by some computational theories of motor control (14, 28). By computing the *z*-scores of kinematic trajectories and by tracking how they changed over the time course of movement, using Spearman's decorrelation and the zero-crossing rate, we show that the motor system can plan a kinematic trajectory which can be guided by internal feedback control. Further, by examining the temporal changes in decorrelation over the trajectory we showed that trajectory control is most prominent during the initial and final phases of the movement.

Materials and Methods

Experiment 1 – Individual cyclic flexion-extension movement of fingers

A detailed description of the experiment can be found in our previously published article (29). In brief, participants sat on a height-adjustable chair and positioned their right dominant arm at ~30^0 shoulder flexion and ~120^0 elbow extension as they rested their forearm

and palm on a flat surface in neutral (pronation-supination) forearm posture (Fig. S1A). The forearm and the thumb were constrained by a strap while the other four fingers of interest were suspended in air and free to move. The movements of phalanges of all four fingers were recorded using electromagnetic tracking sensors (Micro Sensor 1.8^{TM}, Liberty tracking system, Polhemus Inc., Colchester, VT, USA). The task was designed on LabVIEW (National Instruments Corp, Austin, TX, USA) and the data was sampled at a frequency of 100 Hz. A total of eight healthy right-handed subjects (5 males) participated in this study. The experiment was approved by the institute ethics committee at IIT Madras, and all the participants provided a written informed consent before the start of the experiment.

On any given attempt, the subjects were required to maintain a predefined wrist posture (0^0 neutral, 30^0 flexion or 30^0 extension) and asked to make cyclic flexion-extension movements (0.75 Hz movement frequency) at the metacarpophalangeal joint with one of the instructed fingers (among index, middle, ring, and little) between 75±10% of its maximum flexion-extension limits and to ignore any movements in the non-instructed fingers. For this analysis, we considered movements performed by instructed finger as goal-directed and the movements in non-instructed finger as non-goal condition. Each attempt lasted for 32s with an initial 2s of rest followed by 30s of cyclic flexion-extension movements (Fig. S1B). Real-time visual feedback of the distal phalange of the instructed finger was provided on the screen, along with its movement landmarks, and an audio metronome was played at 1.5 Hz to ensure the amplitude and timing of the instructed finger movement, respectively. There were 36 attempts (3 wrist postures x 4 instructed fingers x 3 attempts each) in total. Data from the distal phalanges of each of the four fingers at neutral wrist posture (0^0) were used in this study. Specifically, each attempt was segmented into several half-cycles comprising of movements from flexion (local peaks of middle finger trace in Fig. S1B) to subsequent extension (local troughs of middle finger trace in Fig. S1B) of instructed finger and the same time stamps were

115 used to segment the movements of non-instructed fingers. The half cycles were then resampled
116 to 100 equal spaced segments for analysis in Fig. 2 and the first 300 ms were used for the
117 analysis on actual timing.

118

119 **Experiment 2,3 – Horizontal reaching movements by dominant and non-dominant arms**
120 **and fast and slow movements**

121 Participants: Twenty-five healthy right-handed subjects (15 subjects for experiment 2,
122 and 10 subjects for experiment 3; 21 males; Age [min-max]: 21-32) participated in the study.
123 The experiment was approved by the institute ethics committee at IISc Bengaluru, and all the
124 participants provided a written informed consent before the start of the experiment. The
125 Edinburgh Handedness Inventory (30) was used to evaluate their dominant arm.

126 Experimental Setup: Subjects were made to sit on a chair with a backrest to minimize
127 the movements of the clavicle (collar bone) and their dominant or the non-dominant arm was
128 required to rest on a smooth elevated table to facilitate horizontal reaching movements (Fig.
129 S2A). They were mounted with five electromagnetic 3D motion tracking sensors (Teardrop
130 Mini sensors, 240Hz, Liberty tracking system, Polhemus Inc., Colchester, USA) on the surface
131 of the skin at the sternoclavicular joint (neck), right or left acromion process (right or left
132 shoulder) depending on the task of interest, lateral epicondyle (lateral aspects of the elbow),
133 dorsal tubercle of radius (wrist) and the dorsal aspect of the hand respectively, by a 3M
134 micropore surgical tape. The sensor on the dorsal side hand was used for the current analysis.
135 The lights were switched off in the experimental room to occlude the subject's vision of their
136 arm posture during the movement. Subjects were required to hold an endpoint robotic
137 manipulandum (KINARM, 240 Hz, BKIN Technologies Ltd., Kingston, Canada) and perform
138 a center out discreet horizontal planar reaching movement as required by the task. During the

139 reaching movement, the subjects were required to look at the stimulus screen (LCD Screen, 60
140 Hz) in front of them where a circular shaped cursor on the screen was mapped onto the position
141 of the held manipulandum. All the experimental protocols were coded and executed on
142 TEMPO/VideoSYNC Software (Reflective Computing, St. Louis, MO, USA). The dataset was
143 post-processed using MATLAB interface (MathWorks, Massachusetts, USA).

144 Task Structure: A white fixation box (hollow square, 2cm) appeared at the center of the
145 workspace where the subjects were required to position the pink-colored cursor inside it by
146 moving the manipulandum with one of their arms (Fig. S2B). Once they fixated at the center
147 for 500 ms, a red-colored target (filled square, 1cm) appeared on the screen at an eccentricity
148 of 12 cm from the center at any of the 8 directions (0^0, 45^0, 90^0, 135^0, 180^0, 225^0, 270^0, or 315^0).
149 Subjects made smooth unperturbed goal directed movement towards the target location as soon
150 as the central fixation box disappeared, which was after a delay period of 1000ms. After
151 initiating the movement, they were given 1000ms to reach the target location. Once they
152 reached the target, they were required to stay there for 500ms to successfully complete one
153 trial. The successful completion of the trial was indicated to the subjects by providing a beep
154 sound. The intertrial interval was set to 1500ms where the cursor had to be brought back to the
155 center of the screen in the absence of a stimulus and wait for the next trial. These were
156 considered as non-goal movements as there was no target location and they were not rewarded
157 for the movement (31). Sample movement traces of goal and non-goal conditions by dominant
158 arm and the goal directed movements by non-dominant arm are shown in Fig. S2C. If the
159 subject did not fixate enough at the center or at the target, or if they were not able to execute
160 movements within the required time, the trial was aborted. The experiment was conducted such
161 that 40 successful trials were recorded in each of the 8 directions. The same task was now
162 repeated with the other arm and that the sequence of recruitment of the arms were randomized
163 across subjects to study differences between dominant and non-dominant arms. Experiment-3

164 on fast and slow movements was designed similarly with some minor modifications. The target
165 color was used to cue the subjects about the speed of movement – green for fast (within 400ms)
166 and red (from 600-1000ms) for slow movements and that the trials were randomly interleaved.
167 For this experiment, the subjects used their dominant right arm and performed movements
168 towards 0^0 and 45^0 directions only.

169 Data pre-processing: The motion data from the Polhemus sensor on the hand was low-
170 pass filtered with a cut-off frequency of 20 Hz using a fourth order zero lag Butterworth filter
171 (32). The time at which the hand crossed 5% of its maximum speed during the acceleration and
172 deceleration phases respectively were noted (29, 33, 34). The time of onset and the end of
173 movement were identified by descending along the velocity curve from the 5% mark to
174 whenever it reached zero for the first time. The motion data was then resampled to 100 equally
175 spaced segments to normalize for time across various trials in analysis of Fig. 3, and 4, and the
176 data for the first 500ms during the movement was used for the analysis of actual timing in Fig.
177 3D.

178

179 **Data analysis**

180 The displacement data (in the direction of flexion- extension) of the four fingers (index,
181 middle, ring, and little) from experiment 1 (29), the displacement in X and Y directions
182 (horizontal movement) of the hand from experiment 2 and experiment 3 were used for the
183 analysis. The number of trials in each of the fingers were selected such that the initial postural
184 variability was equated between the goal and the corresponding non-goal fingers. For the goal
185 and non-goal whole-arm movements, the initial variability in hand postures were equated along
186 both X and Y co-ordinates of each of the directions of movement (Fig. S2D). For dominant
187 and non-dominant arm movements, the equalization of initial variability was performed by

188 considering similarity of movements with respect to both arms. For example, the initial
189 variability along 0^0 directed movements by dominant arm were equated with the 180^0 directed
190 movements performed by the non-dominant arm (note that 13 out 15 subjects were analyzed
191 for differences across arms as 2 of them lacked enough number of trials). The initial variability
192 was similar for fast and slow movements as the trials were randomly interleaved. The
193 equalization of initial variability was done to eliminate the influence of initial variance on the
194 decorrelation analysis and restricted to report differences in decorrelation caused due to
195 differences in movement execution.

196 For any given task, and at every normalized time point, each trial was assigned a z-
197 score by subtracting its amplitude from the mean and divided it by the inter-trial standard
198 deviation (Fig. S3). Subtraction from the mean was performed to track how the trajectories
199 across different trials moved relative to the average trajectory, and that they were normalized
200 by the standard deviation, as it changed through the course of movement (Fig. S6A). A sample
201 of movement trajectories (grey) of the arm, directed towards 0^0, is shown in Fig. S3A and the
202 *z*-scores of the corresponding red and blue trajectories are shown in Fig. S3B. The motivation
203 of this procedure was to analyze the within trial variability by observing changes in the *z*-scores
204 of each trial along the duration of movement by providing a unitless geometric approach to
205 study such variability.

206 To investigate the structure of within trial variability we performed Spearman's rank
207 correlation between the *z*-scores at the start of movement $z(0)$, with the *z*-scores at subsequent
208 time instances $z(i)$. In Fig. 1, we have depicted two distinct cases of trajectory control. On the
209 left side (Fig. 1A), the representative trajectories crossover each other such that their relative
210 ranks change during the movement. For example, the rank order of trajectories - red, green,
211 blue, and pink (top to bottom) at time $t = 0$, changes to green, pink, red, and blue at time $t = i$.
212 This leads to decorrelation among their ranks and a decrease in Spearman's correlation

coefficient (ρ), suggesting for the implementation of active trajectory control, which is intended to follow an average trajectory. Conversely, on the right side (Fig. 1B), the order of trajectories remains the same throughout the movement and that the trajectories never converge towards their average trajectory, thereby resulting in high ρ (close to 1) and weaker/lack of implementation of such trajectory control. We perform the decorrelation analysis from movement onset to the end of movement (t = 0 to 100%), to obtain a time varying trajectory of correlation coefficient, $\rho(t)$. We chose the Spearman's correlation coefficient as we were particularly interested in the crossovers among trajectories, independent of changes in inter-trial standard deviation (Fig. S6A) during the time course of movement. To indicate as to why this analysis provides novel insights as compared to that of previous studies (21, 35, 36), we performed the decorrelation analysis between any of the time points with the end of movement for goal and non-goal conditions (Fig. S7). We investigated the average decorrelation ($\bar{\rho}$) over the entire movement duration to quantify the extent of control. We then fit a logistic function $\rho fit(t)$, over the trajectories of $\rho(t)$ for each of the subjects and used parameter β to quantify the rate of decrease of $\rho(t)$ using Eq. 1.

$$\rho fit(t) = a + \frac{1}{1+e^{\beta(\rho(t)-\mathrm{c})}} \quad (1)$$

To substantiate our hypothesis, we computed a dispersion measure for the time normalized trajectories ($A_{n \times T}$, where A represents the amplitude of trajectories with n trials and T = 101, number of normalized time instances) by taking the ratio of average inter-trial standard deviation over the time course, with the average range of movement during the n trials, in Eq. 2. We divided variability with the range, to account for differences in movement amplitude in the finger experiment. We then correlated the average decorrelation ($\bar{\rho}$) with its

average dispersion measure (or with maximum standard deviation in Fig. 3B) expecting that a reduction in $\bar{\rho}$ leads to lower trajectory dispersion.

$$Dispersion = \frac{\frac{1}{T}\sum_{j=1}^{T}\sqrt{\frac{\sum_{i=1}^{n}\left(A_{i,j}-\mu_j\right)^2}{n-1}}}{\frac{1}{n}\sum_{i=1}^{n}\left|\max(A_i)-\min\left(A_i\right)\right|} \quad (2)$$

Where μ_j is the average of amplitude (A) across n trials at time j.

In Fig. S3B, the z = 0, represents an average trajectory (dashed line), and the red trajectory crosses the dashed line three times showing a strong trajectory control while the blue does not cross the dashed line at all showing weaker trajectory control. To quantify this effect, we computed a zero-crossing rate (*ZCR*) from the z-scores of movement trajectories, which was defined as per Eq. 3. A zero-crossover was considered valid only if the amplitude of transition (Δz) at the time of cross-over was greater than 0.01. The threshold was chosen as the *ZCR* under this value did not yield significant differences between goal and non-goal conditions and can be attributed to noise. For arm movements, the *ZCR* plotted in Fig. 3 was further averaged across X and Y co-ordinates and along all the movement directions.

$$ZCR = \frac{Total\ number\ of\ valid\ zero\ crossings}{Total\ number\ of\ trials} \quad (3)$$

To further support the evidence of trajectory control, the starting postures of goal movements in fingers (Fig. S5A) and arm (Fig. S5B), were divided into two groups, the ones which were farther away ($|z| > 0.5$, blue) and the ones closer ($|z| <= 0.5$, black) to the average initial posture (z = 0). The average z-scores (across trials) were tracked along the time course of movement to check the propensity of these two groups to converge towards an average

planned trajectory (z = 0, from time 0 – 100 %). If the central nervous system intended to follow an average trajectory, the group which was farther away from the initial posture should show greater convergence towards the average trajectory than the closer ones. The difference in z-scores at 0th (initial) and 20th percentile time points were used to quantify this effect.

For Fig. 2E and 3F, the decorrelation analysis was performed using a similar technique described earlier but between subsequent 10 % - time instances. At any percentage time point, the value of ρ was computed between the z-scores of trajectories at that time point with respect to an earlier 10%-time instance. At t = 0, ρ was equal to 1, as comparison was made between the z-scores of initial postures with itself, as a reference.

Statistics

The data were checked for normality using the Kolmogorov-Smirnov test. We performed pairwise t-test for paired comparisons and two-sample t-test for independent comparisons if the data were normal, and Wilcoxon signed rank test and Wilcoxon rank-sum test for paired and independent comparisons otherwise. For more than two sample paired comparisons, we performed a repeated measures ANOVA. Multiple pairwise comparisons were reported with Bonferroni corrections.

Results

Trajectory control of goal and non-goal finger movements

The differences in the magnitude of control among goal and non-goal fingers were quantified by computing the average decorrelation ($\bar{\rho}$) during the movement (Fig. 2A). A two-way repeated measures ANOVA (4 finger-tasks x 2 finger-type, goal or non-goal) showed that the $\bar{\rho}$ of goal finger was significantly different from the non-goal finger ($P < 0.001$). By

comparing goal and the corresponding non-goal fingers in a pairwise method it was observed that the extent of decorrelation was highest in the goal fingers (Table S1).

The dynamics of control in goal and non-goal fingers were teased apart by computing the rate of decrease (β) in correlation co-efficient, $\rho(t)$ (Fig. 2A). A logistic function was fitted to the dataset to find β (median explained variance = 0.95). A two-way repeated measures ANOVA (4 finger-tasks x 2 finger-types, goal or non-goal) showed that the rate of decrease of $\rho(t)$ was significantly different across goal and non-goal fingers ($P < 0.001$). Broadly, by performing pairwise comparisons, it was found that the rate of decrease of $\rho(t)$ in the goal directed finger was significantly higher than the non-goal non-neighboring fingers but was from different from that of neighboring fingers (Table S2).

Further, we checked if the average decorrelation in finger trajectories was systematically associated with the average trajectory dispersion (Fig. 2B) and found that they were tightly correlated (Spearman's $\rho = 0.9$, $P < 0.001$), and the average dispersion of goal finger (median = 0.073) was significantly less than that of non-goal neighboring (median = 0.143, $P < 0.001$) and non-neighboring (median = 0.573, $P < 0.001$) fingers (Fig. 2B). Thus, a higher degree of trajectory decorrelation was associated with lesser dispersion in trajectories and vice versa. As goal fingers were associated with varying movement amplitudes, we compared $\rho(t)$ of all four goal fingers to check the sensitivity of the decorrelation analysis to the differences in the range of movement among them (Fig. S4). A one-way repeated measures ANOVA revealed that the $\bar{\rho}$ (Fig. S4B) were not significantly different ($P = 0.72$) and the rate of decrease of $\rho(t)$ (Fig. S4C) were also not significantly different across the goal fingers ($P = 0.52$) but the range of movement (Fig. S4D) were significantly different between them ($P < 0.001$), with index (mean ± SEM: 10.63 ± 0.27 cm) and little (mean ± SEM: 7.42 ± 0.27 cm) fingers having the highest and lowest movement ranges, respectively.

302 We then tested the zero-crossing rate (*ZCR*) of goal and non-goal fingers during the
303 four different instructed finger tasks to probe the propensity of trajectories to follow an average
304 trajectory (Fig. 2A and Fig. S3 for the method of computation). A two-way repeated measures
305 ANOVA (4 finger-tasks x 2 finger-type, goal or non-goal) revealed that the *ZCR* of goal finger
306 was significantly different from that of non-goal fingers ($P < 0.001$). By performing pairwise
307 comparison between goal and non-goal fingers it was found that the goal finger had the highest
308 *ZCR* in all the four tasks (Table S3). To support this further, we divided initial postures of goal
309 fingers into two groups (Fig. S5A), the ones farther away ($|z| > 0.5$, blue) and the ones closer
310 ($|z| <= 0.5$, black) to the average initial posture ($z = 0$) and found that the away group had a
311 significantly greater propensity to converge towards an average trajectory than the closer ones
312 ($P < 0.001$).

313 Next, we quantified the differences in the time of control by performing the
314 decorrelation analysis on the actual timing, from movement onset to 300 ms into the movement.
315 We found that $\rho(t)$ of the goal finger (dark purple) diverged significantly from that of non-goal
316 neighboring (medium purple) and non-neighboring (light purple) fingers at 50ms and 30ms,
317 respectively (Fig. 2D).

318 Motivated by the previous findings, we examined whether trajectory control was
319 continuous or occurred in distinct phases along the movement duration. For this, we performed
320 the decorrelation analysis on the goal finger movements on consecutive 10% - time instances
321 and found that the controller acted discreetly with two prominent troughs in $\rho(t)$ at 20th
322 (binominal $P < 0.001$) and 90th percentile time (binominal $P < 0.001$) points (Fig. 2E)
323 suggesting the presence of early and late phases of control. To substantiate the above finding,
324 we computed the *ZCR* of goal finger movements across three movement segments; early (0 to
325 33 %), middle (34 to 66 %), and late (67 to 100 %) phases of movement duration and found
326 that the *ZCR* was significantly higher during early (mean ± SEM: 0.42 ± 0.01) and late (0.47 ±

0.01) phases as compared to the middle phase (0.25 ± 0.02; $P < 0.001$ for both the comparisons). Also, it was found that the early phase of control (trough at 20 % - 0.78 ± 0.02) was not significantly different from that of late phase (trough at 90 % - 0.77 ± 0.03, $P = 0.69$).

Trajectory control of goal and non-goal whole-arm movements

We investigated whether the above analysis could be extended to whole-arm reach movements and if there were systematic changes in trajectory control for goal and non-goal movements (Fig. 3; see methods and Fig. S2 for a description of goal and non-goal movements). We performed the decorrelation analysis (Fig. 3A) and found that $\bar{\rho}$ in goal movements (mean ± SEM: 0.38 ± 0.02) was significantly less than that of non-goal movements (0.41 ± 0.01, $P = 0.04$; Fig. S6C). This difference in $\bar{\rho}$ was prominent in the first 50 % of the movement duration (goal: 0.5 ± 0.02, non-goal: 0.61 ± 0.01, $P < 0.001$). Like the results from finger experiment, the $\bar{\rho}$ in goal movements was significantly associated with their respective average trajectory dispersion (Pearson's $r = 0.53$, $P = 0.002$, Fig. S6B) and that the trajectory dispersion of goal directed movements (mean ± SEM: 0.168 ± 0.003) was significantly less than that of non-goal movements (0.177 ± 0.003, $P = 0.002$, Fig. S6D). A logistic function was fit over $\rho(t)$ (median explained variance = 0.97) to find the rate of decrease (β) and it was found to be significantly higher in goal movements (mean ± SEM: 0.143 ± 0.05) than the non-goal movements (0.099 ± 0.006, $p < 0.001$).

As expected, the maximum inter-trial standard deviation of goal movements (mean ± SEM: 1.17 ± 0.05 cm) was significantly less than the non-goal movements (1.46 ± 0.05 cm, $P < 0.001$, Fig. 3B and S6A). We wanted to check if this difference in variability could be explained by differences in decorrelation between goal and non-goal movements during the early phases of movement. The $\bar{\rho}$ during the first 20 % - time duration was significantly less in goal movements (mean ± SEM: 0.81 ± 0.01) than the non-goal movements (0.91 ± 0.01, $P <$

352 0.001) and found that it was significantly associated with the maximum standard deviation
353 (Pearson's $r = 0.464$, $P = 0.009$) which occurred much later during the movement (Fig. S6A).
354 Interestingly, this association was conserved for the duration as early as 10 % into the
355 movement execution (Pearson's $r = 0.426$, $P = 0.018$).

356 We also computed the zero-crossing rate (*ZCR*) for goal and non-goal arm movements
357 and found that the *ZCR* of goal movements (mean ± SEM: 1.48 ± 0.03) was significantly greater
358 than the non-goal movements (1.32 ± 0.02; $P < 0.001$, Fig. 3C). Similar to analysis in the
359 previous section, we divided initial postures of goal movements into two groups (Fig. S5B),
360 the ones farther away ($|z| > 0.5$, blue) and the ones closer ($|z| <= 0.5$, black) to the average
361 initial posture ($z = 0$) and found that the away group had a significantly greater propensity to
362 converge towards an average trajectory than the closer ones ($P < 0.001$).

363 To estimate the time of divergence between $\rho(t)$ of goal from non-goal movements, the
364 decorrelation analysis was done on actual time scale, from start to 500 ms into the movement
365 (Fig. 3D) and we observed that they diverged at a median time of 16.67 ms across subjects
366 (Fig. 3E). Further, the maximum change in $\rho(t)$ for goal movements (mean ± SEM: 128.33 ±
367 5.62 ms) and was significantly earlier than for non-goal movements (201.38 ± 8.02 ms, $P <$
368 0.001). These differences between goal and non-goal movements were not because of
369 movement kinematics as the maximum movement speeds were similar across the conditions
370 ($P = 0.62$, Fig. S2E).

371 Further, to investigate whether the controller was continuous or discrete, we performed
372 the decorrelation analysis of goal directed movements on consecutive 10 % - time instances.
373 As was observed for finger movements, we found two distinct troughs at 20th (binomial $P <$
374 0.001) and around 90th (trough shared between 80th and 90th percentiles, binomial $P < 0.001$ for
375 both time stamps, shared across the participants) percentile time instances, indicating early and
376 late phase of control respectively (Fig. 3F). Subsequently, the *ZCR* of goal directed arm

377 movements were computed across three movement segments; early (0 to 33 %), middle (34 to
378 66 %), and late (67 to 100 %) phases of movement duration and found that the *ZCR* was
379 significantly higher during early (mean ± SEM: 0.57 ± 0.01) and late (0.52 ± 0.01) phases as
380 compared the middle phase (0.38 ± 0.05; $P < 0.001$ for both the comparisons), similar to that
381 of finger movements. Also, the trough during early phase of control (mean ± SEM: 0.78 ± 0.01)
382 was significantly less than that of the late phase (0.82 ± 0.01, $P < 0.001$).
383
384 **Invariance in the extent of decorrelation across arms and for different speeds**
385 We tested the decorrelation analysis across dominant and non-dominant arms to see if
386 there were systematic changes in trajectory control with acquisition of skill (Fig. 4A and Fig.
387 S2 for methods). We found that the trajectories overlapped to a large extent and that the $\bar{\rho}$ of
388 dominant arm (mean ± SEM: 0.36 ± 0.02) was not significantly different from that of the non-
389 dominant arm (0.39 ± 0.02, $P = 0.11$, Fig. 4B) and the average effect size was small (Cohen's
390 *d* - 0.34).
391 Next, we subjected the decorrelation analysis to different movement speeds, between
392 fast and slow conditions (Fig. 4C and Fig. S2 for methods) to check how sensitive decorrelation
393 analysis was to differences in signal dependent noise that was expected to be greater for high
394 movement speeds. We found that $\rho(t)$ for fast and slow movements were largely overlapping
395 and that the $\bar{\rho}$ for fast movements (mean ± SEM: 0.44 ± 0.03) was not significantly different
396 from that of slow movements (0.46 ± 0.05, $P = 0.377$, Fig. 4D) and the average effect size was
397 small (Cohen's *d* - 0.49).
398 Taken together, the decorrelation analysis was sensitive to presence or absence of a
399 goal in finger and whole-arm reaching movements, but it was invariant to changes in skill or
400 speed of movement.
401

Discussion

In this study, we used the rate of zero crossings around a mean trajectory as a proxy of trajectory control, and the time course of decorrelation between the initial and subsequent time points as a measure of control and compared these measures in the context of goal and non-goal movements to show that 1) the CNS plans an average trajectory during goal-directed finger and whole-arm reach movements. 2) Trajectory control was found to act at two distinct phases: at early (20 %) and late (around 90 %) phases along the time course of movement. 3) The control (or corrections) in trajectories was initiated as rapidly as 30 ms in goal-directed finger movements and 16.6 ms in goal-directed whole-arm reach movements, providing behavioral evidence for internal feedback control during normative movements.

Relation to previous studies

Since Woodsworth (37), the detailed analysis of the kinematics of limb trajectories has provided insights to understand the relative contributions of motor planning from feedback control (38–41). In addition to assessing the ability of the motor system to regulate variability throughout the trajectory (42), the coefficient of determination (R^2) has been used before as a within-trial estimate of the extent to which early kinematic markers (20, 40, 43, 44) such as peak acceleration and peak velocity determine end-point distributions. In this context, online control has been inferred by measuring the extent to which such markers do not predict the endpoint (i.e., lower R^2). Although inferential, such claims have been validated by manipulating factors such as the availability of visual feedback (45). The decorrelation analysis used in this study uses a similar logic with some important differences that allowed us to reveal novel aspects of trajectory control. First, the earliest kinematic markers typically used are peak acceleration which being (~150 ms) is too late to reveal fast feedback control. Here, in contrast

426 to previous works (35, 44, 46) that have emphasized the relationship of kinematic markers to
427 the end of movement, we measured how quickly trajectories diverged from an initial starting
428 posture. This analysis was facilitated by ensuring that the starting variability between goal and
429 non-goal movements were the same and that any difference in control would be revealed at the
430 earliest possible time. Performing decorrelation analysis with respect to the initial posture was
431 critical to demonstrate effects of fast feedback control as the decorrelation analysis with respect
432 to the end of movement was not sensitive to differences in the early half of the movement that
433 we wanted to address in this paper (Fig. S7). Further, the comparison with non-goal
434 movements that have distinct neural correlates at least in the context of saccade movements
435 (31), as well distinct variability profiles (Fig. S6A) was particularly useful, since it did not
436 involve manipulation of target locations (11, 47) or postures(48, 49) that would emphasize
437 differences in sensory feedback control as opposed to internal feedback control. In this context,
438 although the lack of any difference in the decorrelation profiles between dominant and non-
439 dominant arms was surprising to us given the previous literature (50–53), both tasks were
440 primarily goal driven. Thus, the use of goal and non-goal movements was an important factor
441 to reveal differences in trajectory control using the decorrelation analysis. Also, systematic
442 differences between goal and non-goal condition suggest that the crossovers were not merely
443 because of the phenomenon of regression towards the mean, as both movements started with
444 the same initial variability. Second, in previous studies it is unclear whether to attribute the
445 lack of explained variability to trajectory compensation or to signal dependent noise as well as
446 to nonlinearities that would affect R^2 estimates. Here, the latter potential confound was
447 mitigated using a Spearman's correlation, while the former potential confound was addressed
448 by showing correlations between the early decorrelation signal and trajectory dispersions. Also,
449 if the decorrelation was susceptible to noise, it should have been greater for non-goal
450 movements, while we found that it was the other way round. Finally, the absence of any

difference in the extent of decorrelation for fast versus slow movements suggests that signal-dependent noise per se was not a factor.

Trajectory control during goal-directed movements

Although the notion of a straight-line trajectory plan derives from behavioral studies (3, 4, 54), this notion has been questioned in the context of optimal feedback control models that are able to predict realistic trajectories even in the absence of cost functions that don't involve trajectory specifications (27, 55, 56). Further, the demonstration of relatively fast task-related sensory feedback control (~50 ms) (48, 57) which could in principle shape trajectories during voluntary movement execution involving active participation of motor cortex (26) also is key prediction of optimal feedback control models. However, since movement in optimal feedback models is driven by costs associated with the current posture and the target position, they don't necessarily require movements to crossover an average trajectory. This is in contrast with our observations of zero crossings, which suggest the presence of a mean planned trajectory computed from the initial fixation to the target location. The presence of zero crossings is unlikely to be a consequence of noise since they are more robustly expressed in goal directed finger and whole-arm movements, despite normalizing for the initial postural variability. Thus, we believe the relative paucity of zero crossings and lower decorrelation primarily reflects the absence of robust trajectory control due to the absence of a visual target in non-goal movements.

The other important aspect we tested is whether the CNS implements a fixed extent control along the movement duration or if it is time varying. Modelling of perturbation studies on arm movements has suggested that the extent of feedback controller gains are low near movement initiation while they increase towards the end of movement as the hand reaches the

target (27). In our study, however, we found that there were two distinct phases of control which is reflected at time points where there is a relatively large change of decorrelation, which was in the (Fig 2E and 3F), the early (trough at 20th percentile) and late (trough at 90th percentile) phases. This pattern is reminiscent of virtual via-point control (22) and further reinforces the notion of a mean trajectory that can be efficiently corrected at two extreme postural positions when the velocities of movements are relatively low and state estimation is more robust. Such distinct troughs were not observed in a previous study since the initial variability was clamped and no accuracy constraints were enforced towards the end of movement (35). Further, while implementing control close to the target location is obviously beneficial and has been known since the time of Bernstein's seminal experiments (58), having a high degree of control earlier on has the obvious advantage of clamping variability to manageable levels before the system is swamped by signal-dependent noise. Indeed, we observed that the initial 10 % and 20 % of the response is predictive of the subsequent trajectory variability (Fig. 3B). However, the relative absence of any decorrelation between the early and late phases of control suggests that trajectory control is intermittent. In this context, the absence of trajectory control during the middle phase of the movement is consistent with the predictions of optimal control that don't require explicit trajectory control.

Internal feedback control vs fast sensory feedback control

One of the critical aspects that we addressed in this work is the timing of feedback control that have bearing on the nature of control signals that enable normative goal directed movements. Several studies have indicated signatures of relatively fast feedback control involving reflexive arm movements that occur between 50 – 100 ms after the beginning of movements (26, 44, 48) during tasks that require posture stabilization following mechanical

perturbations. However, whether these feedback signals are also at play during voluntary goal-directed movements is still not clear. On the other hand, internal feedback control implements corrections to trajectories using an efference copy of the initiated motor command (19) to estimate the hand position via a forward model in the absence of delays associated with sensory feedback (59). However, to the best of our knowledge internal feedback has been shown to occur when goals and decisions are changed during movements (24, 43, 60, 61) and help in fast error corrections. In the context of normative movements such internal feedback control has been only studied in the context of fast saccadic eye movements using a similar decorrelation analysis (21). Evidence of internal feedback control has been shown in isometric force application (20) but it has not been demonstrated in normative voluntary reaching movements. In our study, the initiation of control was indexed as the time point when significant differential decorrelations were observed between goal and non-goal movements, and this occurred as early as 30 ms in voluntary finger movements and at 16.6ms for voluntary whole-arm reach movements. We interpret this rapid control in reach movements to be a signature of internal feedback control. However, this early phase of decorrelation was followed with a later stage that is consistent with fast feedback control with peaks at ~94 ms for goal finger and ~128 ms for goal movements of arm (49).

References

1. P. Morasso, Spatial control of arm movements. *Experimental Brain Research* **42** (1981).

2. S. W. Keele, Movement control in skilled motor performance. *Psychological Bulletin* **70**, 387–403 (1968).

3. D. A. Rosenbaum, “Motor Programming: A Review and Scheduling Theory” in *Motor Behavior: Programming, Control, and Acquisition*, H. Heuer, U. Kleinbeck, K.-H. Schmidt, Eds. (Springer, 1985), pp. 1–33.

4. J. P. R. Dick, R. Benecke, J. C. Rothwell, B. L. Day, C. D. Marsden, Simple and complex movements in a patient with infarction of the right supplementary motor area. *Movement Disorders* **1**, 255–266 (1986).

5. M. E. Morris, J. J. Summers, T. A. Matyas, R. Iansek, Current Status of the Motor Program. *Physical Therapy* **74**, 738–748 (1994).

6. J. J. Summers, J. G. Anson, Current status of the motor program: Revisited. *Human Movement Science* **28**, 566–577 (2009).

7. D. W. Moran, A. B. Schwartz, Motor cortical representation of speed and direction during reaching. *J Neurophysiol* **82**, 2676–2692 (1999).

8. C. Padoa-Schioppa, C.-S. R. Li, E. Bizzi, Neuronal Correlates of Kinematics-to-Dynamics Transformation in the Supplementary Motor Area. *Neuron* **36**, 751–765 (2002).

9. M. M. Churchland, G. Santhanam, K. V. Shenoy, Preparatory activity in premotor and motor cortex reflects the speed of the upcoming reach. *J Neurophysiol* **96**, 3130–3146 (2006).

10. P. Cisek, Preparing for Speed. Focus on "Preparatory Activity in Premotor and Motor Cortex Reflects the Speed of the Upcoming Reach." *Journal of Neurophysiology* **96**, 2842–2843 (2006).

11. D. M. Wolpert, Z. Ghahramani, Computational principles of movement neuroscience. *Nature Neuroscience* **3**, 1212–1217 (2000).

12. D. M. Wolpert, M. Kawato, Multiple paired forward and inverse models for motor control. *Neural Networks* **11**, 1317–1329 (1998).

13. D. M. Wolpert, Z. Ghahramani, M. I. Jordan, An internal model for sensorimotor integration. *Science (New York, N.Y.)* **269**, 1880–2 (1995).

14. Desmurget, Grafton, Forward modeling allows feedback control for fast reaching movements. *Trends in cognitive sciences* **4**, 423–431 (2000).

15. E. Bizzi, N. Accornero, W. Chapple, N. Hogan, Posture control and trajectory formation during arm movement. *J. Neurosci.* **4**, 2738–2744 (1984).

16. S. H. Scott, Optimal feedback control and the neural basis of volitional motor control. *Nature Reviews Neuroscience* **5**, 532–546 (2004).

17. E. Todorov, M. I. Jordan, Optimal feedback control as a theory of motor coordination. *Nature neuroscience* **5**, 1226–35 (2002).

18. M. Desmurget, S. Grafton, Feedback or feedforward control: End of a dichotomy. *Taking action: Cognitive neuroscience perspective on intentional acts*, 289–338 (2003).

19. M. Kawato, *et al.*, "Internal forward models in the cerebellum: fMRI study on grip force and load force coupling" in *Progress in Brain Research*, Neural Control of Space Coding and Action Production., (Elsevier, 2003), pp. 171–188.

20. J. Gordon, C. Ghez, Trajectory control in targeted force impulses. III. Compensatory adjustments for initial errors. *Exp Brain Res* **67**, 253–269 (1987).

21. B. A. Richardson, A. Ratneswaran, J. Lyons, R. Balasubramaniam, The time course of online trajectory corrections in memory-guided saccades. *Exp Brain Res* **212**, 457–469 (2011).

22. E. Todorov, M. I. Jordan, Optimal feedback control as a theory of motor coordination. *Nature Neuroscience* **5**, 1226–1235 (2002).

23. D. M. Wolpert, J. Diedrichsen, J. R. Flanagan, Principles of sensorimotor learning. *Nature Reviews Neuroscience* **12**, 739–751 (2011).

24. V. Gaveau, *et al.*, On-line modification of saccadic eye movements by retinal signals. *NeuroReport* **14**, 875 (2003).

25. M. Kawato, Internal models for motor control and trajectory planning. *Current Opinion in Neurobiology* **9**, 718–727 (1999).

26. J. A. Pruszynski, *et al.*, Primary motor cortex underlies multi-joint integration for fast feedback control. *Nature* **478**, 387–390 (2011).

27. D. Liu, E. Todorov, Evidence for the Flexible Sensorimotor Strategies Predicted by Optimal Feedback Control. *J. Neurosci.* **27**, 9354–9368 (2007).

28. C. M. Harris, D. M. Wolpert, Signal-dependent noise determines motor planning. *Nature* **394**, 780–784 (1998).

29. N. Chakrabhavi, V. Skm, Wrist Posture Does Not Influence Finger Interdependence. *J Appl Biomech* **35**, 410–417 (2019).

30. R. C. Oldfield, The assessment and analysis of handedness: The Edinburgh inventory. *Neuropsychologia* **9**, 97–113 (1971).

31. N. Sendhilnathan, D. Basu, M. E. Goldberg, J. D. Schall, A. Murthy, Neural correlates of goal-directed and non–goal-directed movements. *Proceedings of the National Academy of Sciences* **118**, e2006372118 (2021).

32. J. P. Scholz, G. Schöner, M. L. Latash, Identifying the control structure of multijoint coordination during pistol shooting. *Experimental Brain Research* **135**, 382–404 (2000).

33. S. H. Scott, P. L. Gribble, K. M. Graham, D. W. Cabel, Dissociation between hand motion and population vectors from neural activity in motor cortex. *Nature* **413**, 161–165 (2001).

34. A. P. Georgopoulos, J. F. Kalaska, R. Caminiti, J. T. Massey, On the relations between the direction of two-dimensional arm movements and cell discharge in primate motor cortex. *J. Neurosci.* **2**, 1527–1537 (1982).

35. S. Kuang, A. Gail, When adaptive control fails: Slow recovery of reduced rapid online control during reaching under reversed vision. *Vision Research* **110**, 155–165 (2015).

36. M. Krüger, A. Straube, T. Eggert, The Propagation of Movement Variability in Time: A Methodological Approach for Discrete Movements with Multiple Degrees of Freedom. *Frontiers in Computational Neuroscience* **11** (2017).

37. R. S. Woodworth, Accuracy of voluntary movement. *The Psychological Review: Monograph Supplements* **3**, i–114 (1899).

38. R. A. Abrams, D. E. Meyer, S. Kornblum, Eye-hand coordination: Oculomotor control in rapid aimed limb movements. *Journal of Experimental Psychology: Human Perception and Performance* **16**, 248–267 (1990).

39. R. A. Abrams, J. Pratt, Rapid Aimed Limb Movements: Differential Effects of Practice on Component Submovements. *Journal of Motor Behavior* **25**, 288–298 (1993).

40. L. G. Carlton, Processing visual feedback information for movement control. *Journal of Experimental Psychology: Human Perception and Performance* **7**, 1019–1030 (1981).

41. R. Chua, D. Elliott, Visual regulation of manual aiming. *Human Movement Science* **12**, 365–401 (1993).

42. M. A. Khan, *et al.*, Inferring online and offline processing of visual feedback in target-directed movements from kinematic data. *Neuroscience & Biobehavioral Reviews* **30**, 1106–1121 (2006).

43. M. Desmurget, *et al.*, Updating Target Location at the End of an Orienting Saccade Affects the Characteristics of Simple Point-to-Point Movements. *Journal of Experimental Psychology: Human Perception and Performance* **31**, 1510–1536 (2005).

44. J. Messier, J. F. Kalaska, Comparison of variability of initial kinematics and endpoints of reaching movements. *Exp Brain Res* **125**, 139–152 (1999).

45. M. A. Khan, I. M. Franks, Online Versus Offline Processing of Visual Feedback in the Production of Component Submovements. *Journal of Motor Behavior* **35**, 285–295 (2003).

46. B. A. Richardson, A. Ratneswaran, J. Lyons, R. Balasubramaniam, The time course of online trajectory corrections in memory-guided saccades. *Exp Brain Res* **212**, 457–469 (2011).

47. V. Gritsenko, J. F. Kalaska, Rapid online correction is selectively suppressed during movement with a visuomotor transformation. *J Neurophysiol* **104**, 3084–3104 (2010).

48. J. A. Pruszynski, I. Kurtzer, S. H. Scott, Rapid Motor Responses Are Appropriately Tuned to the Metrics of a Visuospatial Task. *Journal of Neurophysiology* **100**, 224–238 (2008).

49. J. A. Pruszynski, *et al.*, Primary motor cortex underlies multi-joint integration for fast feedback control. *Nature* **478**, 387–390 (2011).

50. R. L. Sainburg, D. Kalakanis, Differences in control of limb dynamics during dominant and nondominant arm reaching. *J Neurophysiol* **83**, 2661–2675 (2000).

51. R. L. Sainburg, S. Y. Schaefer, Interlimb Differences in Control of Movement Extent. *Journal of Neurophysiology* **92**, 1374–1383 (2004).

52. R. L. Sainburg, Evidence for a dynamic-dominance hypothesis of handedness. *Exp Brain Res* **142**, 241–258 (2002).

53. X. Xiao, H. J. Hu, L. F. Li, L. Li, Comparison of dominant hand to non-dominant hand in conduction of reaching task from 3D kinematic data: Trade-off between successful rate and movement efficiency. *Math Biosci Eng* **16**, 1611–1624 (2019).

54. P. Morasso, Spatial control of arm movements. *Experimental Brain Research* **42** (1981).

55. V. Vasudevan, A. Gopal, S. Jana, R. Padhi, A. Murthy, Velocity tracking control best explains the modulation of saccade kinematics during eye–hand coordination. *European Journal of Neuroscience* **58**, 2232–2247 (2023).

56. B. Berret, A. Conessa, N. Schweighofer, E. Burdet, Stochastic optimal feedforward-feedback control determines timing and variability of arm movements with or without vision. *PLOS Computational Biology* **17**, e1009047 (2021).

57. D. M. Wolpert, R. C. Miall, M. Kawato, Internal models in the cerebellum. *Trends in Cognitive Sciences* **2**, 338–347 (1998).

58. R. Bongaardt, O. G. Meijer, Bernstein's Theory of Movement Behavior: Historical Development and Contemporary Relevance. *Journal of Motor Behavior* **32**, 57–71 (2000).

59. M. Desmurget, S. Grafton, Forward modeling allows feedback control for fast reaching movements. *Trends in Cognitive Sciences* **4**, 423–431 (2000).

60. L. Pisella, *et al.*, An "automatic pilot" for the hand in human posterior parietal cortex: toward reinterpreting optic ataxia. *Nat Neurosci* **3**, 729–736 (2000).

61. S. B. LoTemplio, *et al.*, Updating the relationship of the Ne/ERN to task-related behavior: A brief review and suggestions for future research. *Frontiers in Human Neuroscience* **17** (2023).

Figures

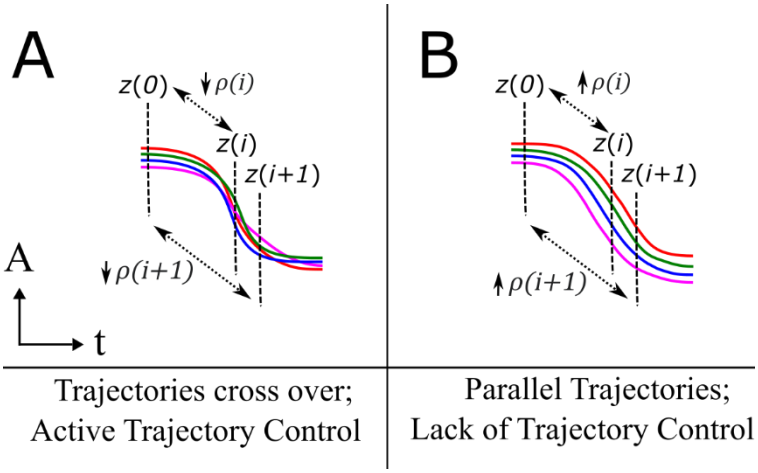

Figure 1: A behavioural signature of active trajectory control. The colors red, blue, green, and pink represent individual trials of a given task. A) If the CNS has a trajectory plan (an average trajectory) that it intends to follow during the task, the *z*-scores at the start of the movement $z(0)$, is posited to change along the time course ($z(i)$ at any time $t = i$), due to the implementation of trajectory control. The crossover among trajectories is captured by a decrease in the Spearman's correlation coefficient (ρ). By performing the decorrelation analysis between movement onset and the subsequent time instances $t = 0,\ldots,i,i+1,\ldots T$ (where T is the end of movement), we obtain a time varying $\rho(t)$. A low value of ρ indicates greater trajectory control and such control also entails trajectories to have lower trajectory dispersion. The extent of trajectory control can also be captured by counting the number of zero-crossings in the *z*-scores, and that it would be more when the system implements a greater degree of control. B) A case where the CNS does not follow an average trajectory. The correlation coefficient ρ remains high and closer to 1 along the time course, accompained with a greater trajectory dispersion and lesser zero crossings.

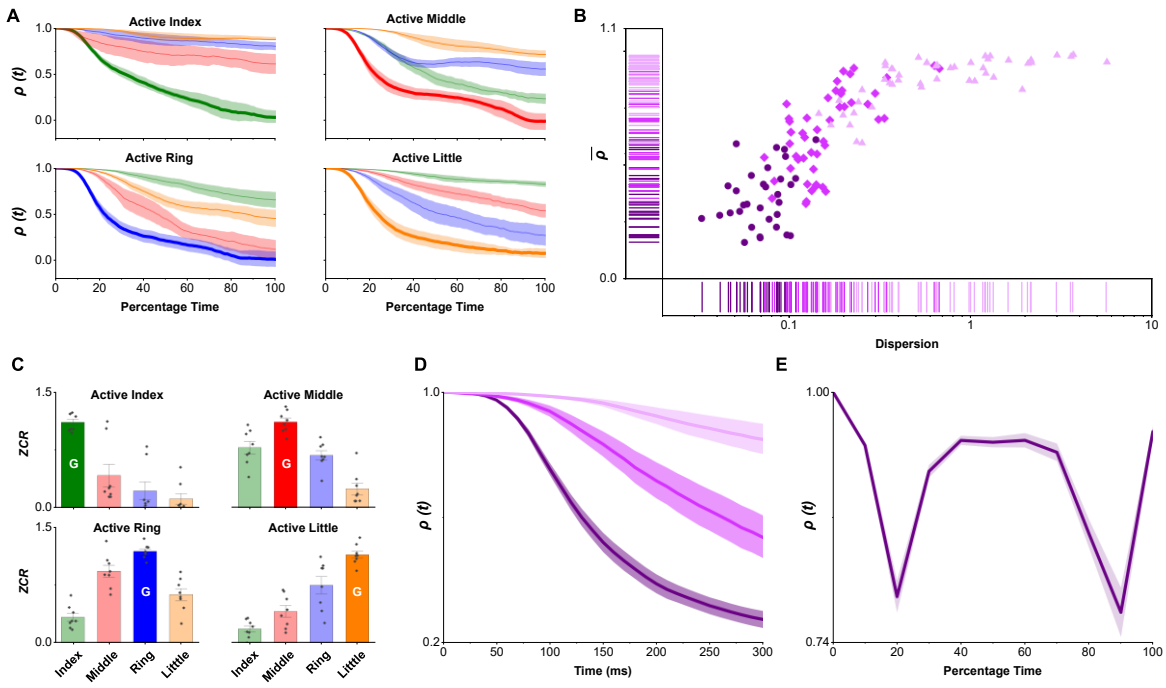

Figure 2: Decorrelation analysis of goal (bold) and non-goal finger movements. A) The trajectories of correlation co-efficient *ρ(t)* of the goal directed index, middle ring, and little finger tasks (mean ± SEM). The decrease in *ρ(t)* is significantly higher in the goal finger of any task. B) Plot of average decorrelation ($\bar{\rho}$) vs average trajectory dispersion shows that the goal fingers (circles) had the lowest $\bar{\rho}$ and lowest trajectory dispersion followed by that of non-goal neighboring fingers (diamonds) and non- neighboring (triangles) fingers. C) The zero-crossing rate (*ZCR*) computed from *z*-scores of goal and non-goal fingers (mean ± SEM) during goal directed index, middle, ring, and little finger tasks. *ZCR* was the highest in the goal finger of any task (further details in the Results, letter G on the bar represents the corresponding goal finger during any task). D) The trajectories of *ρ(t)* (mean ± SEM) of goal finger, and non-goal neighboring and non-neighboring fingers plotted from movement onset to 300ms into the movement. The *ρ(t)* in goal fingers significantly deviated from neighboring and non-neighboring fingers at 50ms and 30ms, respectively. E) Decorrelation analysis of goal finger between consecutive 10%-time instances. The two distinct phases of control, early control at 20% and late control at 90% of movement duration were observed. Color in Fig. A and C: green-index, red-middle, blue-ring, and orange-little fingers. Colors in Fig. B, D and E: dark, medium, and light shades of purple represent goal, non-goal neighboring and non-goal non-neighboring fingers respectively.

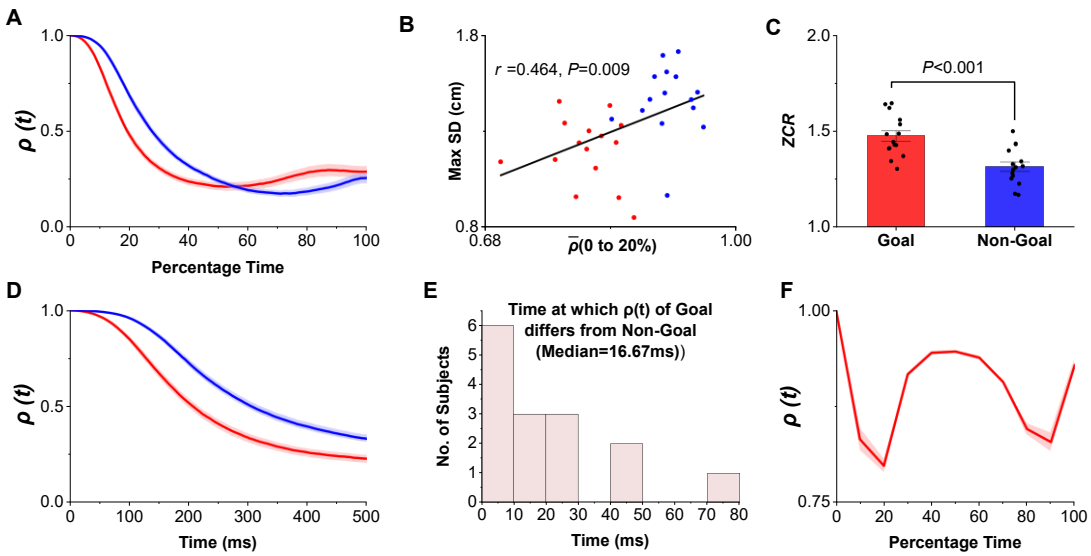

Figure 3: Decorrelation analysis of goal (red) vs non-goal reach movements (blue). A) The decorrelation trajectories *ρ(t)* of goal and non-goal movements (mean ± SEM). B) Correlation between $\bar{\rho}$, computed from 0 to 20% time, with the maximum inter-trial standard deviation of goal (red) and non-goal (blue) trajectories. The initial decorrelation among trajectories was significantly associated with the maximum inter-trial variability ($r = 0.464$, $P = 0.009$) and that the goal movements had lower $\bar{\rho}$ and lesser trajectory variability than non-goal movements. C) The zero-crossing rate (*ZCR,* mean ± SEM) was significantly greater during goal movements than that of non-goal movements ($P<0.001$). D) The variations in decorrelation trajectories *ρ(t)* on actual time scale from movement onset to 500ms into the movement (mean ± SEM), showed a steeper decrease for goal as compared to non-goal movements. E) Histogram of the time at which the *ρ(t)* of goal movements started diverting from the non-goal movements. The diversion happened very early during the movement (median time =16.67ms). F) Decorrelation analysis of goal movements between consecutive 10%-time instances (mean ± SEM). Two distinct phases of control, early control at 20% and late control at 90% of movement duration were observed.

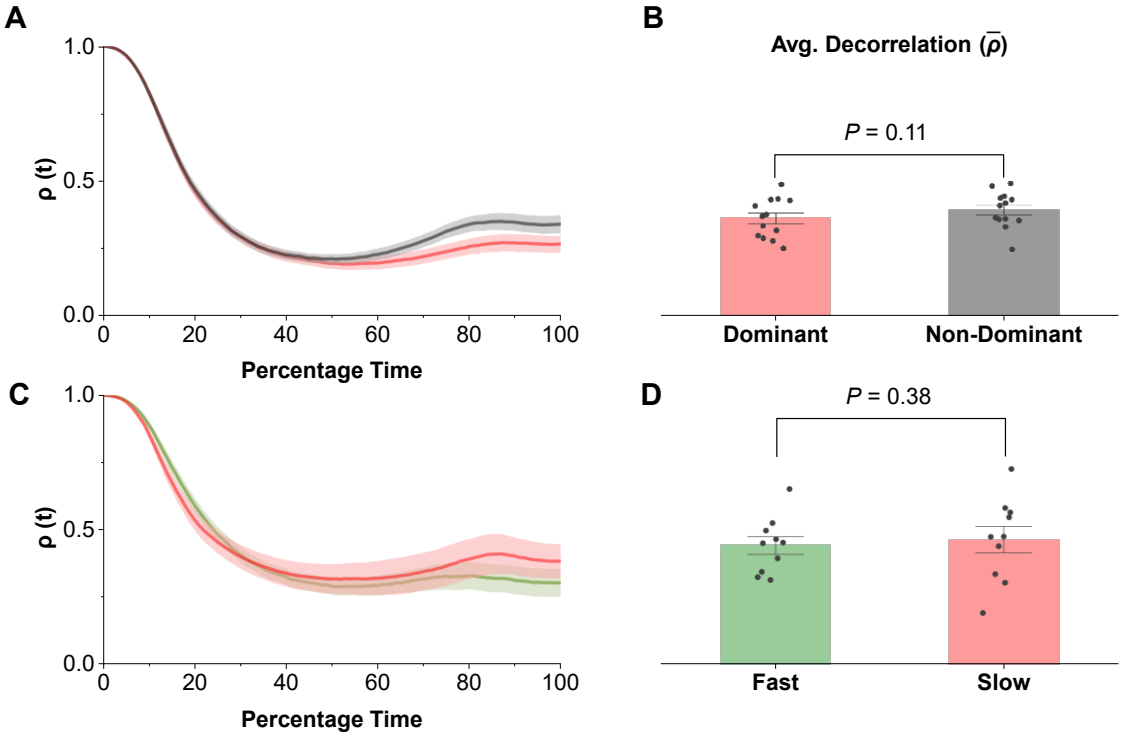

Figure 4: Decorrelation analysis on reaching movements by dominant and non-dominant arms and different movement speeds. A) The decorrelation trajectories $\rho(t)$ (mean ±SEM) of dominant (red) and non-dominant (black) arms. The trajectories were found to overlap along the time course of movement. B) The average decorrelation ($\bar{\rho}$) was not significantly different across dominant and non-dominant arms ($P = 0.11$). C) Plot of $\rho(t)$ trajectories (mean ±SEM) of fast (green) and slow (red) movements by the dominant arm. It was observed that the trajectories overlapped with each other. D) The average decorrelation ($\bar{\rho}$) was not significantly different between fast and slow movements ($P = 0.38$).